

# Probabilistic durability assessment approach of deteriorating RC bridges

Zhu Jinsong<sup>1,2</sup> Gao Change<sup>1</sup>

(<sup>1</sup> School of Civil Engineering, Tianjin University, Tianjin 300072, China)

(<sup>2</sup> Key Laboratory of Coastal Civil Structure Safety of Ministry of Education, Tianjin University, Tianjin 300072, China)

**Abstract:** A stochastic finite element computational methodology for probabilistic durability assessment of deteriorating reinforced concrete (RC) bridges by considering the time- and space-dependent variabilities is presented. First, finite element analysis with a smeared cracking approach is implemented. The time-dependent bond-slip relationship between steel and concrete, and the stress-strain relationship of corroded steel bars are considered. Secondly, a stochastic finite element-based computational framework for reliability assessment of deteriorating RC bridges is proposed. The spatial and temporal variability of several parameters affecting the reliability of RC bridges is considered. Based on the data reported by several researchers and from field investigations, the Monte Carlo simulation is used to account for the uncertainties in various parameters, including local and general corrosion in rebars, concrete cover depth, surface chloride concentration, chloride diffusion coefficient, and corrosion rate. Finally, the proposed probabilistic durability assessment approach and framework are applied to evaluate the time-dependent reliability of a girder of a RC bridge located on the Tianjin Binhai New Area in China.

**Key words:** stochastic finite element method; space-dependent reliability; time-dependent reliability; durability assessment; concrete carbonation; corrosion of rebars

**doi:** 10.3969/j.issn.1003-7985.2011.01.015

Many existing RC bridges are exposed to marine conditions. For these structures, there is an increasing interest in maintaining their safety and serviceability, including their expected remaining life and durability. To date, there are plenty of experimental and theoretical investigations on the deterioration processes of RC bridges in aggressive environments<sup>[1]</sup>. The deterioration processes depend on a large number of variables including concrete properties such as porosity, compression and tensile strength, water/cement ratio, thickness of the concrete cover, reinforcement spacing, quality of concrete constituents, exposure to aggressive agents, and service loading. Many of these are influenced by design, construction workmanship and environments. The deterioration processes are thus highly uncertain. For this reason, probabilistic models are used to characterize the effects of time and space on struc-

tural deterioration<sup>[2-5]</sup>. The reliability and lifetime analyses of existing structures remain a challenging task for computational mechanics.

A stochastic finite element-based computational framework for reliability assessments of deteriorating RC bridges is proposed. The analysis procedure considers the stochastic deterioration processes of concrete, reinforcing steel and the bond between concrete and reinforcing steel. The spatial variability of corrosion damage and its effect on the reliability of RC concrete structures have been studied recently<sup>[6-9]</sup>. Based on the data reported by several researchers and from field investigations, the Monte Carlo simulation is used to account for the uncertainties in various parameters, including local and general corrosion in rebars, concrete cover depth, surface chloride concentration, chloride diffusion coefficients and corrosion rates. The proposed probabilistic durability assessment approach and framework is applied to evaluate the time-dependent reliability of a girder of an RC bridge located at the Tianjin Binhai New Area in China.

## 1 Stochastic Deterioration Model

### 1.1 Concrete degradation model

#### 1.1.1 Carbonation depth model

The depth of carbonation  $x_c$  can be reasonably described by a square root of the time  $t$  relationship<sup>[10]</sup>:

$$x_c(t) = K\sqrt{t} \quad (1)$$

Thus, the evolution of carbonation in time is simply described by the carbonation rate  $K$ , mm/year<sup>0.5</sup>.

It is supposed that corrosion immediately starts when carbonation has attained the rebars. Denoting the concrete cover  $C_{\text{cover}}$ , the time necessary for corrosion to start, called initiation time  $T_{\text{ini}}(1)$ , is<sup>[10]</sup>

$$T_{\text{ini}}(1) = \frac{C_{\text{cover}}^2}{K^2} \quad (2)$$

#### 1.1.2 Concrete constitutive model

In this paper, in agreement with the code of design for concrete structures of China (GB 50010—2002), a constitutive model for concrete with the compression part following a perfectly plastic model and the tension part observing a linear elastic model is adopted<sup>[11]</sup>.

### 1.2 Corrosion-induced deterioration model

#### 1.2.1 Chloride ingress model

For RC bridges, corrosion initiation of reinforcement is normally due to chloride ion ingress. The chloride ion ingress can be modeled using Fick's second law of diffusion:

Received 2010-06-21.

**Biography:** Zhu Jinsong (1975—), male, doctor, associate professor, jszhu@tju.edu.cn.

**Foundation items:** The National Natural Science Foundation of China (No. 50708065), the National High Technology Research and Development Program of China (863 Program) (No. 2007AA11Z113), Specialized Research Fund for the Doctoral Program of Higher Education (No. 20070056125).

**Citation:** Zhu Jinsong, Gao Change. Probabilistic durability assessment approach of deteriorating RC bridges [J]. Journal of Southeast University (English Edition), 2011, 27(1): 70 – 76. [doi: 10.3969/j.issn.1003-7985.2011.01.015]

$$\frac{\partial C}{\partial t} = D_c \frac{\partial^2 C}{\partial x^2} \quad (3)$$

where  $C$  is the chloride ion concentration at distance  $x$  (cm) from the concrete surface,  $\text{kg}/\text{m}^3$ ;  $t$  is the time of exposure to the chloride source, year; and  $D_c$  is the chloride diffusion coefficient,  $\text{cm}^2/\text{year}$ . The corrosion initiation time is<sup>[12]</sup>

$$T_{\text{ini}}(2) = \frac{C_{\text{cover}}^2}{4D_c} \left[ \text{erf}^{-1} \left( \frac{C_s - C_{\text{cr}}}{C_s} \right) \right]^{-2} \quad (4)$$

where  $T_{\text{ini}}(2)$  is the corrosion initiation time, year;  $C_{\text{cover}}$  is the concrete cover depth, mm;  $C_s$  is the equilibrium chloride concentration at the concrete surface, and  $C_{\text{cr}}$  is the threshold chloride concentration at which corrosion begins.

### 1.2.2 Corrosion rate model

After corrosion of steel bars initiates, it is reported that the cover and the concrete quality affect corrosion rates. The corrosion rate can be predicted as a function of the concrete quality, cover, and time since corrosion initiation<sup>[13]</sup>:

$$i_{\text{corr}}(1) = \frac{27(1 - W/C)^{-1.64}}{C_{\text{cover}}} \quad (5)$$

where  $i_{\text{corr}}(1)$  is the corrosion rate at the start of corrosion propagation,  $\mu\text{A}/\text{cm}^2$ ; and  $W/C$  is the water/cement ratio. Vu and Stewart<sup>[13]</sup> suggested that the corrosion rate can be expressed as a time dependent variable:

$$i_{\text{corr}}(t) = \alpha i_{\text{corr}}(1) (t - T_{\text{ini}})^{\beta} \quad t - T_{\text{ini}} \geq 1 \text{ year} \quad (6)$$

where  $T_{\text{ini}}$  is the time to corrosion initiation,  $T_{\text{ini}} = \min [T_{\text{ini}}(1), T_{\text{ini}}(2)]$ ; and  $\alpha$  and  $\beta$  are constants. If the corrosion rate is constant with time, then  $\alpha = 1$  and  $\beta = 0$ . If the corrosion rate reduces with time, then  $\alpha = 0.85$  and  $\beta = -0.29$ <sup>[13]</sup>.

### 1.2.3 Steel cross-sectional area reduction model

The loss of the cross-sectional area of reinforcing steel and its mechanical behavior depend on the type of corrosion. Two types of corrosion of reinforcing steel in concrete are of concern: general and local pitting corrosion.

If general corrosion is considered, the loss of metal due to corrosion is approximately uniform over the whole surface. The reduction in the diameter of a corroding reinforcing bar  $\Delta D$  (mm) after  $t$  years since corrosion initiation can be estimated as<sup>[14]</sup>

$$\Delta D(t) = 0.0232 i_{\text{corr}}(t) t \quad (7)$$

Assuming that the corrosion current density is the same for a group of  $n$  reinforcing bars of the same diameter  $D_0$ , the cross-sectional area after  $t$  years of general corrosion is

$$A_s(t) = n \frac{\pi [D_0 - \Delta D(t)]^2}{4} \geq 0 \quad (8)$$

Pitting corrosion, in contrast to general corrosion, concentrates over small areas of reinforcement. As a result, a corroding area of a reinforcing bar may be much smaller than the area associated with the measurement of  $i_{\text{corr}}(t)$ . For a group of  $n$  reinforcing bars of the same diameter  $D_0$ , the cross-sectional area after  $t$  years of pitting corrosion can

be estimated as

$$A_s(t) = n \frac{\pi D_0^2}{4} - \sum_{i=1}^n A_{p,i}(t) \geq 0 \quad (9)$$

where  $A_{p,i}(t)$  is the cross-sectional area of a pit at time  $t$  in a reinforcing bar with an initial diameter  $D_0$ . It is assumed that the pit has the configuration indicated in Ref. [15].

### 1.2.4 Changes in the ductility of steel bars

There is general consensus that the mechanical behavior of reinforcing bars gradually changes from ductile to non-ductile (brittle) as corrosion loss increases<sup>[14]</sup>. In the present study, it is conveniently assumed that the complete loss of ductility in corroded reinforcing bars occurs after corrosion loss  $\eta_s$  (which is measured in terms of cross-sectional area loss,  $\eta_s = A_p(t)/A_{\text{stnom}}$ ) exceeds the threshold  $\eta_{s,t}$ . This leads to two types of mechanical behavior dependent on corrosion loss:  $\eta_s \leq \eta_{s,t}$  for ductile behavior and  $\eta_s > \eta_{s,t}$  for brittle behavior.

From the experiments proposed by Zhang et al.<sup>[16]</sup>, it is reasonable to quantify  $\eta_{s,t} = 20\%$  for the deformed steel bars in existing structures. According to the experimental results, the elastic modulus of corroded steel bars is independent of corrosion loss. The elastic-plastic stress-strain relationship for corroded steel using tests of 267 corroded steel bars was investigated by Zhang et al.<sup>[16]</sup>.

The stress-strain relationship is described as

$$\sigma_s = \begin{cases} E_{s0} & \varepsilon_{sc} \leq \frac{f_{yc}}{E_{s0}} \\ f_{yc} & \frac{f_{yc}}{E_{s0}} < \varepsilon_{sc} \leq \varepsilon_{shc} \\ f_{yc} = \frac{\varepsilon_{sc} - \varepsilon_{shc}}{\varepsilon_{uc} - \varepsilon_{shc}} (f_{uc} - f_{yc}) & \varepsilon_{sc} > \varepsilon_{shc} \end{cases} \quad (10)$$

where the yield strength  $f_{yc}$  and the ultimate strength  $f_{uc}$  are computed by

$$f_{yc} = \frac{1 - \alpha_1 \eta_s}{1 - \eta_s} f_{y0} \quad (11a)$$

$$f_{uc} = \frac{1 - \alpha_2 \eta_s}{1 - \eta_s} f_{u0} \quad (11b)$$

The yield strain  $\varepsilon_{syc}$ , the strengthened strain  $\varepsilon_{shc}$  and the ultimate strain  $\varepsilon_{suc}$  of corroded steel bars are

$$\varepsilon_{syc} = \frac{f_{yc}}{E_{s0}} \quad (12a)$$

$$\varepsilon_{shc} = \begin{cases} \varepsilon_{syc} + \left( \varepsilon_{sh0} - \frac{f_{y0}}{E_{s0}} \right) \left( 1 - \frac{\eta_s}{\eta_{s,t}} \right) & \eta_s \leq \eta_{s,t} \\ \varepsilon_{syc} & \eta_s > \eta_{s,t} \end{cases} \quad (12b)$$

$$\varepsilon_{suc} = e^{\alpha_3 \eta_s} \varepsilon_{su0} \quad (12c)$$

Zhang et al.<sup>[16]</sup> recommended that the mean values of  $\alpha_1$ ,  $\alpha_2$  and  $\alpha_3$  be 1.049, 1.119 and  $-2.501$ , respectively. These values are used herein. Their coefficients of variation are all the same (i.e., 0.05) and all three variables are assumed Gaussian.

### 1.3 Bond model

The intact bond-slip model of the CEB-FIP model code 1990 was modified by Val and Chernin<sup>[17]</sup> by taking into account the reduction of the bond strength between concrete and corroding reinforcement due to corrosion of reinforcing steel.

The bond-slip relationship in the CEB-FIP model code 1990 (see Fig. 1) is

$$\tau = \begin{cases} \tau_{\max} \left( \frac{s}{s_1} \right)^\alpha & 0 \leq s \leq s_1 \\ \tau_{\max} & s_1 \leq s \leq s_2 \\ \tau_{\max} - (\tau_{\max} - \tau_f) \frac{s - s_2}{s_2 - s_3} & s_2 \leq s \leq s_3 \\ \tau_f & s \geq s_3 \end{cases} \quad (13)$$

where  $\tau$  is the bond stress;  $s$  is the slip;  $\tau_{\max}$  is the bond strength; and  $\alpha$ ,  $\tau_f$ ,  $s_1$ ,  $s_2$ , and  $s_3$  are the parameters of the model, whose recommended values can be found in CEB-FIP model code 1990.

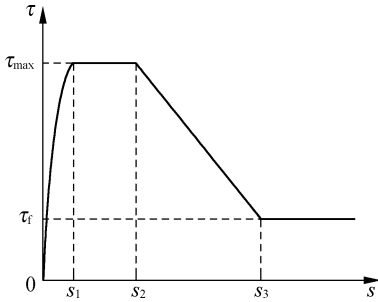


Fig. 1 Bond stress-slip relationship

## 2 Space- and Time-Dependent Reliability Analysis of Deteriorating RC Bridge

### 2.1 Nonlinear finite element model of deteriorated RC bridges

In this paper, a 2-D model with separate elements and nonlinear models for steel, concrete and bond is employed to describe the behavior of deteriorated RC bridges. The concrete is modeled by means of four-node plane stress elements, while the steel bars are represented by two-node truss elements; a bond-link element exhibiting a relative slip between the two materials couples the concrete elements to the corresponding bar elements, as shown in Fig. 2.

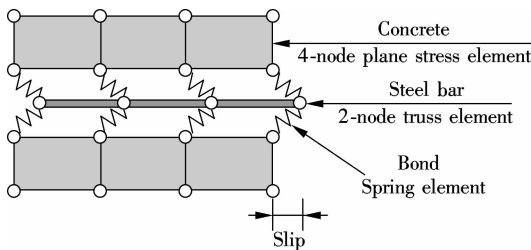


Fig. 2 2-D nonlinear finite element model

### 2.2 Spatial random field analysis

Some of the random input parameters are considered to vary spatially within a particular RC bridge. To illustrate the

techniques developed herein, the present analysis considers the random spatial variability of the concrete cover, the diffusion coefficient and the surface chloride concentration. These variables in turn will influence the spatial variability of dependent variables such as the corrosion initiation time and the corrosion rate. Spatial variability can be represented by the use of random fields; in the case of an RC beam, it is represented by a 1-D random field. To achieve this, the length of beam  $L$  is discretized into  $n$  identical square elements and a random variable is used to represent the random field over each element.

#### 2.2.1 Surface chloride concentration

In the coastal zone, McGee<sup>[18]</sup> suggested that the surface chloride concentration as a function of distance from the coast  $d$  (km) is

$$C_s(d) = \begin{cases} 2.95 & d \leq 0.1 \\ 1.15 - 1.81 \log(d) & 0.1 < d \leq 2.84 \\ 0.03 & d > 2.84 \end{cases} \quad (14)$$

McGee<sup>[18]</sup> found that the coefficient of variation (COV) for surface chloride concentration is 0.49 for distances from the ocean exceeding 0.1 km. In the present study, a coefficient of variation of 0.5 is used.

#### 2.2.2 Chloride diffusion coefficient

The Chinese code specifies that the chloride diffusion coefficient should be determined based on experimental or measured data. It has been observed that there is a tendency for a decrease in the chloride diffusion coefficient over time, but this reduction is most rapid during the first 5 years of exposure, and after that, it approaches a constant value. A wide range of chloride diffusivity rates is found in the literature ranging from 70 to 1350 mm<sup>2</sup>/year<sup>[6]</sup>. In this study, the variation of probabilities of corrosion initiation is examined with time-independent constant diffusion coefficient  $D_c$  of 330 mm<sup>2</sup>/year. The coefficient of the variation of diffusion coefficient for specified concrete compressive strengths of 30 to 40 MPa is approximately 0.45.

#### 2.2.3 Concrete cover depth

Substantial research has been performed on the variability of concrete cover depth. Factors that influence concrete cover depth variability include the complexity of steel fixing, contractor's practice, number of quality checks, formwork erection and concrete casting. The majority of these factors relate to workmanship; thus, based on published data, the distributions assumed for cover depth in the case studies described herein are given in Tab. 1.

### 2.3 Load model

The live load model is based on the Chinese code (JTG D60—2004). The calculated static live load effects are multiplied by a dynamic factor  $\mu$  to account for the dynamic amplification effects. The total live load is then multiplied by an overload factor  $\lambda_L$  to account for the uncertainty in the overload conditions of existing highway bridges. In addition, it is considered that  $\lambda_L$  might be truncated at some lower legal limit, such as the live load in the code.

It is assumed that the maximum annual live load follows a Gumbel (extreme type I) distribution, whereas the dynamic factor  $\mu$  is assumed to be normally distributed. The distri-

butions for the components of the dead load are assumed as log-normal.

**Tab. 1** Statistical properties of random variables

Parameter	Mean	COV	Distribution
Concrete compressive strength $f_c$ /MPa	35	0.18	N
Modulus of elasticity of concrete $E_c$ /GPa	30	0.12	N
$D_0$ /mm	32	0.10	N
$f_{yc}$ /MPa	335	0.10	N
Modulus of elasticity of steel $E_{s0}$ /GPa	200	0.033	N
$C_{cover}$ /mm	50	0.20	LN
$C_s$ (using deicing salt)/(kg · m <sup>-3</sup> )	3.5	0.50	LN
$C_s$ (costal zone)/(kg · m <sup>-3</sup> )	Eq. (14)	0.5	LN
$D_c$ /(mm <sup>2</sup> · year <sup>-1</sup> )	330	0.10	LN
$C_{cr}$ /(kg · m <sup>-3</sup> )	0.9	0.19	LN
$\alpha_1$	1.049	0.05	N
$\alpha_2$	1.119	0.05	N
$\alpha_3$	-2.501	0.05	N
Dead load precast/(kN · m <sup>-1</sup> )	$1.03D_p$	0.08	LN
Dead load cast-in-place/(kN · m <sup>-1</sup> )	$1.05D_c$	0.10	LN
Single truck load/kN	90	0.05	Gumbel
Distributed live load/(kN · m <sup>-1</sup> )	3.97	0.05	Gumbel
Dynamic factor $\mu$	1.24	0.15	N, truncated at 1
Overload factor $\lambda_L$	1.2	0.20	N, truncated at 1

Note:  $D_p$  and  $D_c$  denote the nominal dead loads of precast and cast-in-place, respectively; N and LN denote normal and lognormal distribution.

## 2.4 Limit state function

The limit state function can be written as

$$g(\mathbf{x}, t) = R(t) - S(t) = 0 \quad (15)$$

where  $\mathbf{x}$  is the design variable vector defining limit state function  $g$ , and  $R(t)$  and  $S(t)$  are time-dependent variables representing resistance and load effect, respectively.

The limit states considered herein are serviceability and strength (see Tab. 2). The load effects are calculated by the nonlinear finite element analysis of the deteriorating RC bridges.

**Tab. 2** Time-dependent variables in limit state functions

Limit states	$R(t)$	$S(t)$
Serviceability SE	$L/600$	Maximum deflection at mid-span under live load
Strength ST <sub>1</sub>	$f_y$	Steel tensile stress under combined load
Strength ST <sub>2</sub>	$f_c$	Concrete compression stress under combined load

## 2.5 Computational procedure

The space- and time-dependent reliability analysis is complicated due to nonlinear limit states, time-dependent and random variables, and more importantly, the inclusion of the temporal and spatial variabilities of steel constitutive laws, steel cross-sections and the bond-slip relationship induced by pitting corrosion.

For each simulation, the time to corrosion initiation and the corrosion rate for each steel element are calculated. At each calculation time, the pit-depth for each steel element and the concrete cover depth are generated. The cross-sectional area and constitutive laws of the corroded steel, and the bond-slip relationship between corroded steel and concrete are taken into account. The reinforcing bar forces, compression stress of the concrete, and the displacement at mid-span are then calculated from finite element analysis.

A computer code written in Matlab version R2006a is used to generate the random variable inputs and to conduct the reliability analysis. The software ANSYS and its parametric design language are used to perform the nonlinear finite element analysis of degraded reinforced concrete bridges. The stochastic parameters such as material properties, structural dimensions and element properties are input. The Monte Carlo simulation is used to obtain the failure probabilities and reliability indices<sup>[19]</sup>. The flowchart describing the program structure for spatial time-dependent reliability analysis is shown in Fig. 3.

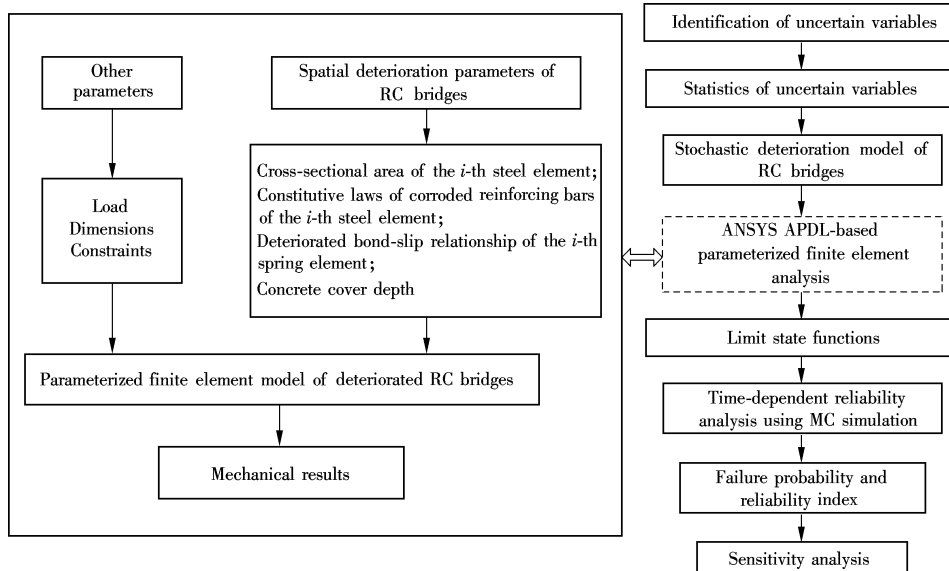


**Fig. 3** Flowchart of space- and time-dependent reliability analysis

### 3 Illustrative Example: Existing RC Bridge on Coastal Environment

#### 3.1 Bridge description

For the sake of illustrating the present model and method, a typical simple supported RC bridge located on the Tianjin Binhai New Area of China is considered herein. The bridge has a span of 20 m and two-lane-roadway and two sidewalks with a total width of 9.5 m. It has five precast T-type RC girders with the geometrical characteristics of the cross-section and the steel reinforcement shown in Fig. 4(a). The bridge was designed according to the Chinese code (JGJ D62—2004) for a highway-II live load. Reinforcing steel is HRB335 and there is a 50 mm thick concrete overlay. The specified concrete compressive strength  $f_c$  of the girder is 35 MPa and the nominal yield strength of the reinforcing

steel  $f_{yc}$  is 335 MPa. Ten reinforcing bars of 32-mm-diameter are used for longitudinal reinforcement, and stirrups are made of 12-mm-diameter rebars. The service life of the structure is taken as 100 years. The bridge is located within 2 km of the coast and is exposed to repeated application of deicing salts in winter. The corrosion rates are evaluated at a relative humidity of 70%. In the present study, one of the side-girders of this bridge is selected for reliability analysis.

A plane stress modeling of the T-type beam is performed by nonlinear finite element simulations. The longitudinal rebars in the 20 m span girder are divided into 200 steel elements and the length of each element is 100 mm. The concrete element length is also 100 mm. The FE model comprises 1 600 concrete elements, 200 steel elements and 400 spring elements. The FE mesh used is defined in Fig. 4(b), and the detailed links between the steel bar and the concrete are shown in Fig. 2.

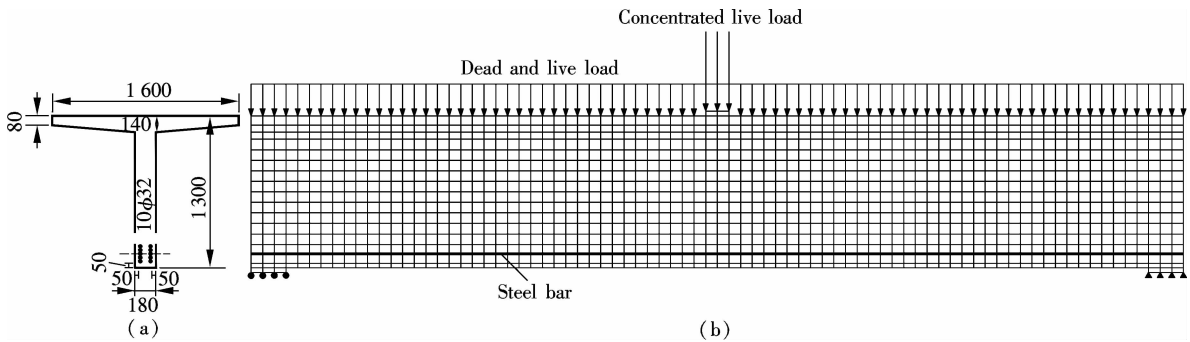


Fig. 4 Reinforced concrete bridge beam. (a) Cross section (unit: mm); (b) 2-D finite element mesh of the beam

In the reliability analysis, structural failure is deemed to occur if the tensile stress of the steel element at mid-span exceeds the ultimate strength of the steel, or the compression stress of the concrete element at the deck exceeds the compression strength of the concrete. Serviceability failure will occur when the maximum deflection of the bridge under live load exceeds 1/600 of its span according to the Chinese code JGJ D62—2004. As mentioned in section 2.4, these failure states are denoted as  $ST_1$ ,  $ST_2$  and SE, respectively. The statistical properties of all the random variables for the space- and time-dependent reliability analysis of this RC bridge are summarized in Tab. 1.

#### 3.2 Results

The time-dependent reliability indices of the beam under different failure criteria are presented in Fig. 5. It shows that

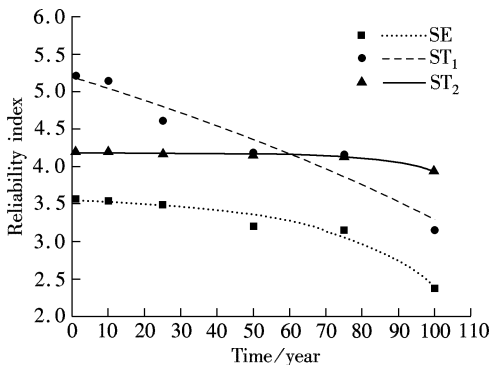


Fig. 5 Time-dependent reliability index of RC bridge

the reliability is significantly influenced by the failure criteria. The probability density functions of the live load deflections at mid-span from 10 to 100 years are illustrated in Fig. 6.

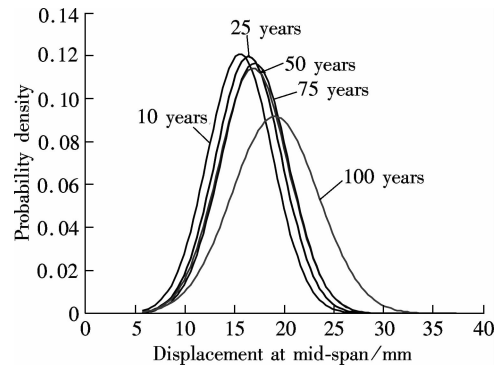


Fig. 6 Probability density functions for live load deflection at mid-span at different bridge ages

Nominal concrete covers for the reinforcing bar are 35 mm (level 1), 50 mm (level 2) and 75 mm (level 3) according to the Chinese code. The mean values of overload factor  $\lambda_L$  are considered as 1.2, 2.0 and 3.0 for common, severe and extreme overload. It is worth noting that the mean cases of  $\lambda_L$  in Tab. 3 are determined according to the surveys on traffic trucks and recent failures of highway bridges in China.

Reliability analyses are conducted to assess the influence of cover on failure probabilities. The effect of concrete cover depth at  $t = 25$  years is illustrated in Fig. 7. According to the durability design code of China, the RC T-type beam

with a cover depth of 50 mm can satisfy the minimum reliability index of 3.5 after 25 years, whereas a design scheme with a 35 mm cover depth cannot.

**Tab. 3** Case of sensitivity analysis

Parameter	Base case	Range of mean values
$C_{\text{cover}}/\text{mm}$	N (50, 10)	35, 50, 75
$\lambda_L$	N (1.2, 0.24)	1.2, 2.0, 3.0

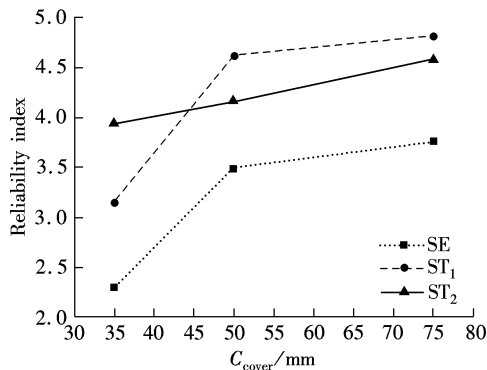


**Fig. 7** Effect of concrete cover depth on 25 years reliability

Fig. 8 illustrates the influences of the overload factor  $\lambda_L$  on the serviceability (live load deflection) and strength (steel tension and concrete compression) probabilities of failure of corroded beam for 25-year deterioration. The reliability indices are significantly affected by the overload factor. According to Fig. 8, for a 25-year RC bridge, the acceptable overload factor is about 1.7.

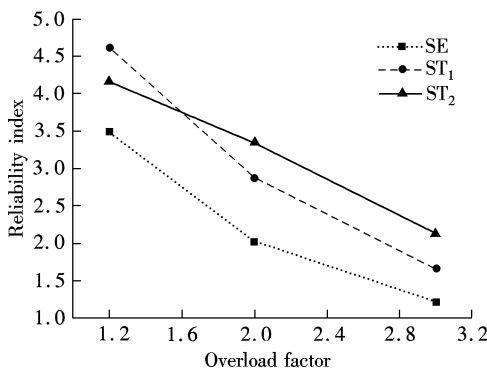


**Fig. 8** Effect of overload factor on 25 years reliability

## 4 Conclusion

Reliability assessment of RC bridges in a marine environment considering the spatial and temporal variabilities of deterioration processes is performed in the present study. A stochastic finite-element-based computational framework for reliability assessment of deteriorating RC bridges is developed. The spatial variabilities of concrete cover, surface chloride concentration and chloride diffusion coefficients are considered. The results obtained from the space- and time-dependent reliability analysis of a RC bridge girder are presented in terms of serviceability and strength limit states. This information can be used to optimize maintenance strategies, and evaluate the time-dependent reliability and residual life of deteriorating RC bridges.

## References

- [1] Biondini M, Frangopol D M. Lifetime reliability-based optimization of reinforced concrete cross-sections under corrosion [J]. *Structural Safety*, 2009, **31**(6): 483–489.
- [2] Enright M P, Frangopol D M. Probabilistic analysis of resistance degradation of reinforced concrete bridges beams under corrosion [J]. *Engineering Structures*, 1998, **20**(11): 960–971.
- [3] Enright M P, Frangopol D M. Service-life prediction of deteriorating concrete bridges [J]. *Journal of Structural Engineering*, 1998, **124**(3): 309–317.
- [4] Marsh P S, Frangopol D M. Reinforced concrete bridge deck reliability model incorporating temporal and spatial variations of probabilistic corrosion rate sensor data [J]. *Reliability Engineering and System Safety*, 2008, **93**(3): 394–409.
- [5] Val D V, Stewart M G. Reliability assessment of ageing reinforced concrete structures—current situation and future challenges [J]. *Structural Engineering International*, 2009, **19**(2): 211–219.
- [6] Stewart M G. Spatial variability of damage and expected maintenance costs for deteriorating RC structures [J]. *Structure and Infrastructure Engineering*, 2006, **2**(2): 79–90.
- [7] Marsh P S, Frangopol D M. Lifetime multi-objective optimization of cost and spacing of corrosion rate sensors embedded in a deteriorating reinforced concrete bridge deck [J]. *Journal of Structural Engineering*, 2007, **133**(6): 777–787.
- [8] Stewart M G, Al-Harthy A. Pitting corrosion and structural reliability of corroding RC structures: experimental data and probabilistic analysis [J]. *Reliability Engineering and System Safety*, 2008, **93**(3): 373–382.
- [9] Stewart M G, Suo Q H. Extent of spatially variable corrosion damage as an indicator of strength and time-dependent reliability of RC beams [J]. *Engineering Structures*, 2009, **31**(1): 198–207.
- [10] Bertolini L. Steel corrosion and service life of reinforced concrete structures [J]. *Structure and Infrastructure Engineering*, 2008, **4**(2): 123–137.
- [11] Ministry of Housing and Urban-Rural Development of the People's Republic of China. GB 50010—2002 Code for design of concrete structures [S]. Beijing: China Architecture & Building Press, 2002. (in Chinese)
- [12] Bastidas-Arteaga E, Bressollette P, Chateaufneuf A, et al. Probabilistic lifetime assessment of RC structures under coupled corrosion-fatigue deterioration processes [J]. *Structural Safety*, 2009, **31**(1): 84–96.
- [13] Vu K A T, Stewart M G. Structural reliability of concrete bridges including improved chloride-induced corrosion models [J]. *Structural Safety*, 2000, **22**(4): 313–333.
- [14] Stewart M G. Mechanical behavior of pitting corrosion of flexural and shear reinforcement and its effect on structural reliability of corroding RC beams [J]. *Structural Safety*, 2009, **31**(1): 19–30.
- [15] Val D V, Melchers R E. Reliability of deteriorating RC slab bridges [J]. *Journal of Structural Engineering*, 1997, **123**(12): 1638–1644.
- [16] Zhang W P, Shang D F, Gu X L. Stress-strain relationship of corroded steel bars [J]. *Journal of Tongji University*, 2006, **34**(5): 184–195. (in Chinese)
- [17] Val D V, Chernin L. Serviceability reliability of reinforced concrete beams with corroded reinforcement [J]. *Journal of Structural Engineering*, 2009, **135**(8): 896–905.
- [18] McGee R. Modeling of durability performance of Tasmanian bridges [C]// *ICASP8 Applications of Statistics and Probability in Civil Engineering*. Sydney, Australia, 1999: 297–306.

[19] Zhu J S, Xiao R C, He L Z. Reliability assessment of large-span cable-stayed bridges based on artificial intelligence[J].

*Journal of China Civil Engineering*, 2007, **40**(5): 41 - 47.  
(in Chinese)

## 退化钢筋混凝土桥梁概率耐久性评估方法

朱劲松<sup>1,2</sup> 高嫦娥<sup>1</sup>

(<sup>1</sup> 天津大学建筑工程学院, 天津 300072)

(<sup>2</sup> 天津大学滨海土木工程结构与安全教育部重点实验室, 天津 300072)

**摘要:**提出了考虑时间、空间变异特性的退化钢筋混凝土桥梁耐久性概率评估的随机有限元方法. 首先, 通过考虑钢筋与混凝土之间时变的粘结滑移关系及腐蚀钢筋的应力应变关系, 采用弥散裂纹方法对退化钢筋混凝土桥梁进行有限元分析. 然后, 提出了退化钢筋混凝土桥梁耐久性概率评估的随机有限元分析方法, 基于文献及现场调查的数据, 采用蒙特卡罗仿真方法对钢筋均匀及点锈蚀、混凝土保护层厚度、表面氯离子含量、氯离子扩散系数及腐蚀率等进行随机抽样, 考虑这些时变及空间变异的因素对钢筋混凝土桥梁可靠度的影响. 最后, 以天津滨海新区的一座钢筋混凝土梁桥为例分析了所提方法的应用.

**关键词:**随机有限元法; 空间相关可靠度; 时间相关可靠度; 耐久性评估; 混凝土碳化; 钢筋锈蚀

**中图分类号:** U448. 34